# An update of IPCC climate reference regions for subcontinental analysis of climate model data: Definition and aggregated datasets

Maialen Iturbide[1], José Manuel Gutiérrez[1], Lincoln Muniz Alves[2], Joaquín Bedia[3], Ruth Cerezo-Mota[4], Ezequiel Cimadevilla[3], Antonio S. Cofiño[3], Alejandro Di Luca[5], Sergio Henrique Faria[6,7], Irina Gorodetskaya[8], Mathias Hauser[9], Sixto Herrera[3], Kevin Hennessy[10], Helene T. Hewitt[11], Richard G. Jones[11,12], Svitlana Krakovska[13,14], Rodrigo Manzanas[15,3], Daniel Martínez-Castro[16,17], Gemma Teressa Narisma[18], Intan S. Nurhati[19], Izidine Pinto[20], Sonia I. Seneviratne[9], Bart van den Hurk[21], and Carolina S. Vera[22]

[1] Grupo de Meteorología. Instituto de Física de Cantabria (CSIC-UC). Santander, Spain

[2] National Institute for Space Research. São José dos Campos, Brazil

[3] Grupo de Meteorología. Dpto. Matemática Aplicada y Ciencias de la Computación. University of Cantabria. Santander, Spain

[4] Universidad Nacional Autónoma de México (UNAM). Mexico city, Mexico

[5] Climate Change Research Centre and ARC Centre of Excellence for Climate Extremes, University of New South Wales. Sydney, Australia

[6] Basque Centre for Climate Change (BC3), Leioa, Spain

[7] IKERBASQUE, Basque Foundation for Science, Bilbao, Spain

[8] Centre for Environmental and Marine Studies Department of Physics, University of Aveiro. Aveiro, Portugal

[9] Institute for Atmospheric and Climate Science, ETH Zurich. Zurich, Switzerland

[10] CSIRO Oceans and Atmosphere. Melbourne, Australia

[11] Met Office Hadley Centre. Exeter, United Kingdom

[12] School of Geography and Environment, University of Oxford. UK

[13] Ukrainian Hydrometeorological Institute. Kyiv, Ukraine

[14] State Institution National Antarctic Scientific Center. Kyiv, Ukraine

[15] Intergovernmental Panel on Climate Change (IPCC), WGI-TSU, Université Paris-Saclay. Paris, France

[16] Instituto de Meteorología de Cuba. La Habana, Cuba

[17] Instituto Geofísico del Perú. Lima, Perú

[18] Manila Observatory, Ateneo de Manila University campus. Quezon City, Philippines

[19] Research Center for Oceanography. Indonesian Institute of Sciences. Jakarta, Indonesia

[20] Climate System Analysis Group (CSAG), University of Cape Town. South Africa

[21] DELTARES. Delft, The Netherlands

[22] Departamento de Ciencias de la Atmósfera y los Océanos, FCEyN-UBA. Centro de Investigaciones del Mar y la Atmósfera (CIMA), Instituto Franco Argentino sobre Estudios de Clima y sus Impactos (UMI IFAECI)/CNRS-CONICET. Buenos Aires, Argentina

**Abstract.** Several sets of reference regions have been used in the literature for the regional synthesis of observed and modelled climate and climate change information. A popular example is the series of reference regions used in the Intergovernmental Panel on Climate Change (IPCC) Special Report on Managing the Risks of Extreme Events and Disasters to Advance Climate Adaptation (SREX). The SREX regions were slightly modified for the 5th Assessment Report of the IPCC and used for reporting sub-continental observed and projected changes over a reduced number (33) of climatologically consistent regions encompassing a representative number of grid boxes. These regions are intended to allow analysis of atmospheric data over broad land or ocean regions and have been used as the basis for several popular spatially aggregated datasets, such as the seasonal mean temperature and precipitation in IPCC regions for CMIP5.

We present an updated version of the reference regions for the analysis of new observed and simulated datasets (including CMIP6) which offer an opportunity for refinement due to the higher atmospheric model resolution. As a result, the number of land and ocean regions is increased to 46 and 15 respectively, better representing consistent regional climate features. The paper describes the rationale for the definition of the new regions and analyses their homogeneity. The regions are defined as polygons and are provided as coordinates and shapefile together with companion R and Python notebooks to illustrate their use in practical problems (e.g. calculating regional averages). We also describe the generation of a new dataset with monthly temperature and precipitation, spatially aggregated in the new regions, currently for CMIP5 and CMIP6, to be extended to other datasets in the future (including observations). The use of these reference regions, dataset and code is illustrated through a worked example using scatter plots to offer guidance on the likely range of future climate change at the scale of the reference regions. The regions, datasets and code (R and Python notebooks) are freely available at the ATLAS GitHub repository; https://github.com/SantanderMetGroup/ATLAS, https://doi.org/10.5281/zenodo.3998463 (Iturbide et al., 2020).

KEY WORDS: *Regional climate change; Climatic regions; CMIP5; CMIP6; Climate change projections; Reproducibility*

## 1 Introduction

Different sets of climate reference regions have been proposed in the literature for the regional synthesis of historical trends and future climate change projections, and have been subsequently used in the different Assessment Reports of the IPCC (we refer to these sets as *IPCC WGI reference regions*). The *Giorgi* reference regions (originally 23 rectangular regions proposed in Giorgi and Francisco, 2000; denoted here as *version 1*) were used in the third (AR3, Giorgi et al., 2001) and fourth (AR4, Christensen et al., 2007) IPCC Assessment reports. These regions were modified using more flexible polygons in the IPCC Special Report on Managing the Risks of Extreme Events and Disasters to Advance Climate Adaptation (SREX, Seneviratne et al., 2012; *version 2*) and then slightly modified and extended to 33 regions (by including island states, the Arctic and Antarctica) for the fifth Assessment Report (AR5, van Oldenborgh et al., 2013; *version 3*), as shown in Figure 1a. The objective in these revisions was to improve the climatic consistency of the regions so they represent sub-continental areas of greater climatic coherency. This process typically resulted in a higher number of smaller regions, constrained by the relatively coarse resolution of the global models, since each region should encompass a sufficient number of gridboxes. The AR5 reference regions (http://www.ipcc-data.org/guidelines/pages/ar5_regions.html; last access: 30 July 2020) were developed for reporting sub-continental CMIP5 projections (with an average horizontal resolution greater than 2°) and were quickly adopted by the research community as a basis for regional analysis in a variety of applications (Bärring and Strandberg, 2018; Madakumbura et al., 2019). Moreover, these regions have been used to generate popular spatially aggregated datasets, such as the *seasonal mean temperature and precipitation in IPCC regions for CMIP5* (McSweeney et al., 2015), which provides ready-to-use information from the CMIP5 models, suitable for regional analysis of climate projections and their uncertainties. This dataset can be directly used by researchers and stakeholders for a variety of purposes, including assessing the internal variability, model and scenario uncertainty components (Hawkins and Sutton, 2009), or assisting in the comparison and selection of representative sub-ensembles for impact studies (e.g., Ruane and McDermid, 2017).

The increasing availability of CMIP6 multi-model simulations (O'Neill et al., 2016; NCC editorial, 2019) offers an opportunity to refine the AR5 reference regions —due to the higher atmospheric model resolution, typically around 1°— and also to produce ready-to-use aggregated regional information for the updated reference regions. This is a timely task due to the great interest of the research community in the higher sensitivity of some CMIP6 models and the potential implications for climate change studies (Forster et al., 2020). Here, we present the results of an initiative carried out during the last year to achieve this goal. First, we present the updated regions (referred to as *IPCC WGI reference regions, version 4*) and describe the rationale for the revision, which was guided by two basic principles: 1) climatic consistency and better representation of regional climate features and 2) representativeness of model results (sufficient number of model gridboxes per region). Climatic homogeneity is characterized in terms of mean temperature and precipitation considering Köppen-Geiger climatic regions (Rubel and Kottek, 2010), the annual cycle and projected changes over the reference regions. The resulting 46 land plus 15 ocean regions (see Figure 1b) are provided as coordinates (in csv format) and also as a shapefile with companion notebooks to illustrate their use in R and Python.

Second, we describe the monthly regional temperature and precipitation dataset obtained by spatially aggregating the model data over the reference regions (currently for CMIP5 and CMIP6, to be extended later to observations and additional datasets). Finally, the use of these reference regions, datasets and code is illustrated through a reproducible example which analyses the likely range of future temperature and precipitation changes that are expected for different European regions using scatter plots.

Section 2 presents the data and methods used in this work. Section 3 describes the reference regions and their rationale. The regionally aggregated CMIP5 dataset is presented in Section 4 and links are provided for additional aggregated datasets (e.g. CMIP6, which are periodically updated); a reproducible illustrative example is described in Section 5. Finally, conclusions and discussion are presented in Section 6.

## 2 Data and Methods

We use global gridded observations to characterize the regional climatological conditions at a sub-continental scale. In particular, we use CRU TS (version 4.03; Harris et al., 2014; Harris and Jones, 2020) providing monthly precipitation and temperature with a resolution of 0.5° over land for the period 1901-2017. Figure 2a-b shows the annual mean temperature and precipitation climatology for the period 1981-2010. CRU TS does not cover Antarctica, which is therefore infilled with an alternative dataset, namely the EWEMBI gridded observations (Lange, 2019). Figure 2c shows the Köppen-Geiger climatic regions (Rubel and Kottek, 2010) computed from these datasets. Quantifying the observational uncertainty is an increasing concern in climate studies, particularly for precipitation (Kotlarski et al., 2019). Therefore, we use two additional observational datasets for precipitation in some parts of this study: 1) Global Precipitation Climatology Centre (GPCC, v2018; Schneider et al., 2011) providing monthly land precipitation values with 0.5° resolution for the period from 1891 to 2016, and 2) Global Precipitation Climatology Project (GPCP; Monthly Version 2.3 gridded, merged satellite/gauge precipitation; Huffman et al., 2009), providing monthly land and ocean precipitation values with a resolution of 2.5° for the period 1979-2018. We show results for the current WMO climatological standard normal period 1981–2010 (WMO, 2017).

Global model scenario data were downloaded for CMIP5 (Taylor et al., 2012)/CMIP6 (O'Neill et al., 2016) models for the historical (1850- 2005/1850-2014) and RCP2.6/SSP1-2.6, RCP4.5/SSP2-4.5 and RCP8.5/SSP5-8.5 future scenarios (2006-2100/2015-2100). Data for CMIP5 (curated version used for IPCC-AR5) was downloaded from the IPCC Data Distribution Center (https://www.ipcc-data.org/sim/gcm_monthly/AR5/ index.html; last accessed, 31 Dec 2019) and for CMIP6 was downloaded from the Earth System Grid Federation (ESGF, Balaji et al., 2018); a periodically updated inventory is available at the ATLAS GitHub repository (in the *AtlasHub-inventory* folder). All model data have been interpolated to common 2° (for CMIP5) and 1° (CMIP6) grids —separately for land and ocean gridboxes using conservative remapping (using CDO with the models and target land/sea masks; CDO, 2019),—

which are typical model resolutions for CMIP5 and CMIP6 models, respectively. The common grids and land/sea masks are available in the ATLAS GitHub repository (in the *reference-grids* folder).

In this paper we illustrate the results using the curated CMIP5 dataset and refer to the ATLAS GitHub repository for similar results for CMIP6. Figure 2d-e shows the CMIP5 multi-model climate change signal for annual mean temperature (in absolute terms) and precipitation (relative, in %) for RCP8.5 2081-2100 (w.r.t. the modern climate baseline 1986-2005 used in AR5). This figure shows the typical spatial climate change patterns and is used to illustrate the consistency of the regional signals in the climate reference regions.

## 3 Reference Regions: Rationale and Definition

The *Giorgi* reference regions were originally defined with the goal to represent consistent climatic regimes and physiographic settings, while maintaining an appropriate size for model representation (thousands of kilometers, to contain several model gridboxes), using some subjectivity in the final selection (Giorgi and Francisco, 2000). Here, we are guided by the same basic principles to define a new version of the reference regions (see Figure 1b). Climatic homogeneity is characterized in terms of mean temperature and precipitation considering Köppen-Geiger climatic regions (see Figure 2) and also the annual precipitation cycle (Figures 3 and 4); in the latter case, observational uncertainty is analysed using the three alternative datasets described in Sec. 2. Representativity of model results (sufficient number of gridboxes per region) is analysed at the end of this section in Figure 5.

### 3.1 Definition of new regions

Here we describe the rationale for the new version of the reference regions presented in this paper (version 4, see Figure 1b) which is based on the latest available version (version 3, see Figure 1a) that was used in AR5. In contrast to the AR5 regions, the new version includes 16 oceanic regions suitable for the analysis of large-scale atmospheric data. Many of the new land regions are defined by splitting the previous ones to increase climatic homogeneity as described below.

In North America, the AR5 Polar Greenland-Iceland (GIC) region is divided in two, Northeastern North America (NEN) and Greenland/Iceland (GIC), to better accommodate the subarctic and Polar climates, respectively (Figure 2c). The eastern and central Northern America regions (ENA and CNA) are maintained mostly unaltered while the western part is reorganized to increase climate consistency. The new Northwestern region (NWN) includes mostly the subarctic regions, whereas the modified western region (WNA) encompasses a variety of regional intermixed climates (semiarid, Mediterranean, and continental; see Figure 2c) which are difficult to further separate due to the complex orography.

The new North Central America (NCA) region includes the semiarid and arid climates of Northern Mexico, separating them from the tropical climates in southern Central America which constitute a new region (SCA). The Caribbean (CAR) region has been modified to fully include the Greater Antilles.

In South America, the AR5 northwestern Amazonia region is divided into three subregions to separate the Northern South America (NSA) region from the western region (NWS) —which includes the northern Andes Mountains range, — and the South America Monsoon (SAM) region. These regions represent sub-continental areas of greater climatic coherency (Espinoza et al 2019), both in terms of climate and climate change signals (Figures 2c-e), and exhibit characteristic seasonal precipitation cycles (Figure 3), with a rainy season from October to March in SAM and no clear wet and dry seasons for NSA and NWS. The Northeastern region is maintained, but the name is changed to Northeastern South America (NES). The old southern South America region is divided in two, separating the northern (southeastern South America, SES) and southern (SSA) parts, the later encompassing the mostly cold desert climates exhibited in this region (see Figure 2c).

The three European reference regions NEU, CEU (renamed Western and Central Europe, WCE) and MED have been maintained unaltered since they encompass the main regional climates in Europe, from subarctic, to oceanic/continental and to Mediterranean. However, an additional region has been introduced in Eastern Europe (EEU), encompassing the continental climate on the western side of the Ural mountain range.

For Africa, the AR5 WAF region has been divided in two (WAF and CAF); although these regions have similar Köppen-Geiger climates (see Figure 2c), they have very different annual cycles (Figure 4) and therefore should be analysed independently (Diedhiou et al., 2018). A similar situation was found in the original EAF (Osima et al., 2018) which was also divided in two, a Northern subregion (NEAF) which includes the arid region of the Horn of Africa, and a Southern subregion (SEAF). These two regions also exhibit different precipitation seasonal cycles, with different timing of the annual maximum (see Figure 4). Moreover, the South Africa region SAF was also divided in subregions with different rainfall regimes (Maúre et al., 2018), the western subregion (WSAF) including the arid regional climates, and the Eastern region (ESAF). Additionally, the (sub)tropical region of Madagascar (MDG) was split from the continent.

In the case of Asia, Northern Asia is subdivided in a Northern subarctic region (RAR), two regions for Western (WSB) and Eastern (ESB) Siberia and a region for the Russian far East (RFE). The original Western Asia region (WAS) is divided in two regions, Western central Asia (WCA) and the Arabian Peninsula (ARP), the later with an arid climate; these two sub-regions exhibit a distinct seasonal cycle (see Figure 4). The old Tibetan plateau (TIB) region is divided in two subregions, separating the highland climate of the Tibetan plateau in the South (TIB) from the northern arid subregion (Eastern Central Asia, ECA). The South Asia (SAS), East Asia (EAS) and Southeast Asia (SEA) are maintained unaltered, with the exception of adjustments caused by changes in neighboring regions and the definition of two ocean regions (the Arabian Sea and the Bay of Bengal) for the oceanic part of the original SAS.

Regarding Australasia, the Southern region (SAU) is now further south, better differentiating the rainfall climatology (Fig. 2c) and separated from the oceanic New Zealand (NZ). The Northern region is divided in three subregions to increase climatic consistency (CSIRO and Bureau of Meteorology, 2015; see Figure 1b) separating the northern tropical region (NAU), the central arid region (CAU) and the subtropical east coast (EAU).

In contrast to the version 3 reference regions used in AR5, those defined in this paper also include 15 oceanic regions (note that the Caribbean, the Mediterranean and South East Asia are considered both land and ocean regions, defined using the land and sea masks, respectively). In version 3 only selected sub-domains of the Indian and tropical Pacific ocean were designated as reference regions and the rest of the main oceanic regions were not represented. Version 4 includes representation of all major oceanic regions. The equatorial and northern and southern extents of each of the main non-polar oceans are defined as separate regions with the added refinement of dividing the “northern Indian ocean” into two, the Arabian Sea and the Bay of Bengal. The Arctic Ocean is defined as the region north of the main Eurasian and North American landmass which then also defines the northern extent of the North Pacific and Atlantic regions. The equatorial regions extend from 10S to 10N to include those regions used to define indices for both El Nino and the Indian Ocean Dipole. The southern extent of the South Pacific, Atlantic and Indian regions are similar to those defined by Durack and Wijffels (2010) with the remaining ocean region to the south defined as a single Southern Oceans region.

Since these ocean regions largely exclude the coastal zones (which are often included in the “land” regions), they are generally more suitable for the analysis of large-scale atmospheric data. Figures 2d and 2e demonstrate that in this respect the ocean regions are a good addition to the AR5 definitions even though they were not developed with the intention of defining ocean basin masks for zonal means used by oceanographers. However, we note that since the coastal regions can be defined by applying a land-sea mask to the land boxes, it is possible to combine regions to enable the more traditional ocean basin definitions used by oceanographers to be produced to a large extent (albeit not exactly).

### 3.2 Representativeness of model results

The higher atmospheric resolution of CMIP6 yields better model representation on the reference regions (more gridboxes per region) allowing a revision for better climatic consistency (e.g. dividing heterogeneous regions) while preserving model representativeness. Figure 5 illustrates this, displaying the number of gridboxes (only land gridboxes for land regions) in each of the AR5 (last column) and revised (first column) reference regions for the two reference grids (1° and 2°), as well as for the CMIP6 model grids (representing the multi-model mean of gribox numbers). This figure shows that the 1° grid provides a good reference for CMIP6. Moreover, it shows that the new reference regions are more representative than the AR5 ones due to the increase of model resolution (see Figures 5a and 5d, corresponding to the cases of CMIP6 data on the updated reference regions, and to CMIP5 data in the original AR5 regions, respectively). The regions with the smallest number of gridboxes correspond to three island regions: The Caribbean (CAR), New Zealand (NZ), and Madagascar (MDG), with around 20-60 gridboxes per region. Note that the updated regions are also suitable for the analysis of CMIP5 data (at 2° resolution, Fig. 5c) since all regions encompass over ten land gridboxes, with the exception of the three above-mentioned regions, where results should be interpreted with caution.

These updated regions are defined as polygons (the lines in Figure 1 are straight lines on a projected plane) and are provided as coordinates and shapefile at the ATLAS GitHub (*reference-regions* folder); the reference grids and land-sea masks can be found at the *reference-grids* folder. Moreover, companion R and Python notebooks are also available (*reference-regions/notebooks*) to illustrate their use in practical problems (e.g. calculating regional averages).

## 4 Regionally Aggregated CMIP Datasets

The seasonal mean temperature and precipitation in CMIP5 models averaged over the version 3 (AR5) reference regions is a popular dataset, suitable for the regional analysis of climate projections and their uncertainties (McSweeney et al., 2015). Here we extend this idea to the new regions and model data and compute aggregated monthly results over the different reference regions (see Figure 1b) for all the CMIP5 simulations (and also the available CMIP6 ones), considering land only, sea only, and land-sea gridboxes (the land/sea masks are available in the ATLAS GitHub repository, *reference-grids*). Results are calculated for each model simulation and stored individually as a text-csv file, with regions in columns (including the global results in the last column) and dates (months) in rows; results for a one ensemble member per model are included directly in the ATLAS Github repository (*aggregated-datasets* folder), and links are provided to the general dataset (full ensemble with all runs) which allows for internal variability studies.

Whereas the aggregated CMIP5 dataset is final, results for CMIP6 will be regularly updated when new data become available at ESGF; these two datasets constitute alternative lines of evidence for climate change studies and the ATLAS initiative presented here facilitates intercomparison of results and consistency checks for the reference climatic regions. Note that although the aggregated data provides summary climate information for each sub-continental region which is useful for a broad spectrum of users, detailed climate information at local or regional scales (in each sub-continental region) would be required for further regional analysis.

## 5 Illustrative Case Study

To demonstrate a potential application of the reference regions and the associated regionally-averaged CMIP data (for temperature and precipitation), we show a simple case study illustrating the projected range of future temperature/precipitation change. This can provide useful context information for a variety of impact and adaptation studies. In particular, we use scatter plots to show the median, 10th, and 90th percentiles of the CMIP5 ensemble change. We focus on three illustrative European regions (NEU, WCE and MED) with opposite climate change signals for precipitation (see Figure 2e). The code and data needed to run this example (which can be extended to other regions, or combination of regions, and datasets, e.g. CMIP6) are all available at the ATLAS GitHub repository (*aggregated-datasets/scripts* folder) and can be run in a local R session accessing the GitHub data with no further requirements.

Figure 6 shows the projected changes in annual mean temperature and precipitation resulting from the script *scatterplots_TvsP.R*. In particular, results from RCP2.6, RCP4.5 and RCP8.5 scenarios for early (2021-2040), mid (2041-2060 and 2061-2080) and late (2081-2100) 21st century — relative to the 1986-2005 baseline period — for each of the three European subregions are displayed. This figure projects an increase of temperature in all European domains —with similar warming in all regions for the different scenarios and future periods— and a consistent meridional gradient of changes in precipitation, with a clear precipitation increase in NEU, non-changing conditions in WCE (uncertainty range crossing the zero line), and reduced precipitation over MED. The same scripts can be applied to the currently available CMIP6 dataset by changing two parameters to check the consistency of these results for the updated models and scenarios.

Note that this illustrative example can be modified to serve different purposes. For instance, the same diagram can be adapted to display the individual model values (or to select the subset of models spanning the uncertainty range) in order to assist in the comparison and the selection of representative sub-ensembles for impact studies (e.g. Ruane and McDermid, 2017). The calculation of the regional aggregated values is time consuming (computed offline and results are provided in the GitHub repository); however, accessing the values and plotting the results is straightforward and the scripts provided run in a few seconds.

## 6 Conclusions and Discussion

A new set of 46 land plus 15 ocean regions is introduced in this work updating the previous set of IPCC AR5-WGI reference regions for the regional synthesis of model-projected climate change information (in particular for the new CMIP6 simulations). The new regions increase the climatic consistency of the previous ones —by rearranging and dividing regions exhibiting mixed regional climates— and have a suitable model representation (the minimum is in the range 20-60 model gridboxes for three particular island regions: the Caribbean, New Zealand and Madagascar.

This revision was guided by the basic principles of climatic consistency and model representativeness, but there is of course some subjectivity in the final selection.

We also present a new dataset of monthly CMIP5/6 spatially aggregated information using the new reference regions and the available CMIP5 (from the IPCC-DDC) and CMIP6 data (from ESGF, as of 30 September 2019), and describe a worked example on how to use this dataset to inform regional climate change studies, in particular about the likely range of future temperature/precipitation changes for the different European reference regions using scatter plots.

## 7 Code and data availability

The present work is part of the climate change ATLAS initiative (which is aligned with IPCC AR6 activities). The definition of the regions, the code and the associated spatially-aggregated datasets are available at the GitHub ATLAS repository: https://github.com/SantanderMetGroup/ATLAS, https://doi.org/10.5281/zenodo.3998463 (Iturbide et al., 2020). The ATLAS project builds in the publicly available climate4R R framework (Iturbide et al., 2019) (available under the GNU General Public License v3.0) and provides additional functions which may be relevant for the users of the reference regions and aggregated datasets, such as the calculation of global warming levels, thus enhancing the functionalities presented in this work. The python notebook is based on the *regionmask* (Hauser, 2019) and xarray (Hoyer and Hamman, 2017) packages, among others. The results for CMIP5 are based on the final curated dataset used for IPCC-AR5, but other datasets will be updated periodically when new data becomes available (e.g. CMIP6, still in progress).

Regarding the original datasets used in this work, all of them are publicly available from the local providers — CRU TS4.03 is distributed under the Open Database License, and EWEMBI and GPCCv2018 are distributed under the Creative Commons Attribution 4.0 International License — and/or the Earth System Grid Federation (ESGF, Balaji et al., 2018) — CMIP5 and CMIP6. Moreover, for the sake of reproducibility some datasets have been also replicated at the Santander Climate Data Service which is transparently accessible from climate4R via the User Data Gateway (registration is required to accept the terms of use of the original datasets; more information at http://meteo.unican.es/udg-wiki, last access: 30 July 2020).

***Author contributions.*** Gutiérrez J.M. and Iturbide M. conceived the study and wrote the code and the manuscript; vandenHurk B. conceived the case study; Iturbide M. and Hauser M. implemented the R and Python companion notebooks; all authors contributed to the definition of the regions, to the discussion and revised the text and the results.

***Competing interests.*** The authors declare that there is not any competing interest.

## Acknowledgements

We acknowledge the World Climate Research Program's Working Group on Coupled Modelling, which is responsible for CMIP, and we thank the climate modeling groups (listed in the Atlas GitHub) for producing and making available their model output.
JMG and SH acknowledge support from the Spanish Government through the research and innovation programme (project ref. PID2019-111481RB-I00) and the María de Maeztu excellence programme (Ref. MdM-2017-0765). SHF acknowledges support from the Spanish Government through the María de Maeztu excellence programme (Ref. MDM-2017-0714), and by the Basque Government through the BERC 2018–2021 programme.
The authors are also grateful to the two reviewers (Chris Brierley and one anonymous) who helped to improve the original manuscript with a detailed in deep revision providing constructive comments, and to Michael Grose and Jason Evans who provided useful comments during the interactive discussion.

## REFERENCES

Balaji, V., Taylor, K. E., Juckes, M., Lawrence, B. N., Durack, P. J., Lautenschlager, M., Blanton, C., Cinquini, L., Denvil, S., Elkington, M., Guglielmo, F., Guilyardi, E., Hassell, D., Kharin, S., Kindermann, S., Nikonov, S., Radhakrishnan, A., Stockhause, M., Weigel, T., and Williams, D.:

Requirements for a global data infrastructure in support of CMIP6, Geoscientific Model Development, 11, 3659–3680, https://doi.org/https://doi.org/10.5194/gmd-11-3659-2018, 2018.

Bärring, L. and Strandberg, G.: Does the projected pathway to global warming targets matter?, Environmental Research Letters, 13, 024 029, https://doi.org/10.1088/1748-9326/aa9f72, publisher: IOP Publishing, 2018.

CDO: Climate Data Operator Version 1.9.8. Max-Planck-Institute for Meteorology, https://code.mpimet.mpg.de/projects/cdo, 2019.

CSIRO and Bureau of Meteorology 2015, Climate Change in Australia Information for Australia's Natural Resource Management Regions: Technical Report, CSIRO and Bureau of Meteorology, Australia. http://www.climatechangeinaustralia.gov.au

Christensen, J., Hewitson, B., Busuioc, A., Chen, A., Gao, X., Held, I., Jones, R., Kolli, R., Kwon, W.-T., Laprise, R., Rueda, V. M., Mearns, L., Menez, C., Rn, J., Rinke, A., Sarr, A., and Whetton, P.: Climate Change 2007: The Physical Science Basis. Contribution of Working Group I to the Fourth Assessment Report of the Intergovernmental Panel on Climate Change [Solomon, S., D. Qin, M. Manning, Z. Chen, M. Marquis, K.B. Averyt, M. Tignor and H.L. Miller (eds.)], book section Regional Climate Projections, pp. 847–940, Cambridge University Press, Cambridge, United Kingdom and New York, NY, USA, 2007.

Diedhiou, A., Bichet, A., Wartenburger, R., Seneviratne, S. I., Rowell, D. P., Sylla, M. B., Diallo, I., Todzo, S., Touré, N. E., Camara, M., Ngatchah, B. N., Kane, N. A., Tall, L., and Affholder, F.: Changes in climate extremes over West and Central Africa at 1.5°C and 2°C global warming, Environmental Research Letters, 13, 065 020, https://doi.org/10.1088/1748-9326/aac3e5, 2018.

Durack, P. J., and S. E. Wijffels, 2010: Fifty-Year Trends in Global Ocean Salinities and Their Relationship to Broad-Scale Warming. J. Climate, 23, 4342–4362, https://doi.org/10.1175/2010JCLI3377.1.

Espinoza, J.C., Ronchail, J., Marengo, J.A. et al. Contrasting North–South changes in Amazon wet-day and dry-day frequency and related atmospheric features (1981–2017). Clim Dyn 52, 5413–5430, 2019. https://doi.org/10.1007/s00382-018-4462-2

Forster, P. M., Maycock, A. C., McKenna, C. M., and Smith, C. J.: Latest climate models confirm need for urgent mitigation, Nature Climate Change, 10, 7–10, https://doi.org/10.1038/s41558-019-0660-0, 2020.

Giorgi, F. and Francisco, R.: Uncertainties in regional climate change prediction: a regional analysis of ensemble simulations with the HADCM2 coupled AOGCM, Climate Dynamics, 16, 169–182, https://doi.org/10.1007/PL00013733, 2000.

Giorgi, F., Hewitson, B., Christensen, J., Hulme, M., Storch, H. V., Whetton, P., Jones, R., Mearns, L., and Fu, C.: Climate Change 2001: The Scientific Basis [J. T. Houghton, Y. Ding, D. J. Griggs, M. Noguer, P. J. vad der Linden, X. Dai, K. Maskell, C. A. Johnson (eds.)], book section Regional Climate Information?Evaluation and Projections, pp. 583–638, Cambridge University Press, 2001.

Harris, I. and Jones, P.: CRU TS4.03: Climatic Research Unit (CRU) Time-Series (TS) version 4.03 of high-resolution gridded data of month-by-month variation in climate (Jan. 1901- Dec. 2018), Centre for Environmental Data Analysis, https://doi.org/http://dx.doi.org/10.5285/10d3e3640f004c578403419aac167d82, 2020.

Harris, I., Jones, P. D., Osborn, T. J., and Lister, D. H.: Updated high-resolution grids of monthly climatic observations – the CRU TS3.10 Dataset, International Journal of Climatology, 34, 623–642, https://doi.org/10.1002/joc.3711, 2014.

Hawkins, E. and Sutton, R.: The Potential to Narrow Uncertainty in Regional Climate Predictions, Bulletin of the American Meteorological Society, 90, 1095–1108, https://doi.org/10.1175/2009BAMS2607.1, 2009.

Hoyer, S. and Hamman, J., 2017. xarray: N-D labeled Arrays and Datasets in Python. Journal of Open Research Software, 5(1), p.10. DOI: doi:10.5334/jors.148.

Huffman, G. J., Adler, R. F., Bolvin, D. T., and Gu, G.: Improving the global precipitation record: GPCP Version 2.1, Geophysical Research Letters, 36, https://doi.org/10.1029/2009GL040000, 2009.

Iturbide, M., Bedia, J., Herrera, S., Baño-Medina, J., Fernández, J., Frías, M. D., Manzanas, R., San-Martín, D., Cimadevilla, E., Cofiño, A. S., and Gutiérrez, J. M.: The R-based climate4R open framework for reproducible climate data access and post-processing, Environmental Modelling & Software, 111, 42–54, https://doi.org/10.1016/j.envsoft.2018.09.009, 2019.

Iturbide, M., Gutiérrez, J. M., Cimadevilla, E., Bedia, J., Hauser, M., and Manzanas, R.: SantanderMetGroup/ATLAS GitHub (Version v1.6), https://doi.org/10.5281/zenodo.3998463, 2020.

Kotlarski, S., Szabó, P., Herrera, S., Räty, O., Keuler, K., Soares, P. M., Cardoso, R. M., Bosshard, T., Pagé, C., Boberg, F., Gutiér- rez, J. M., Isotta, F. A., Jaczewski, A., Kreienkamp, F., Liniger, M. A., Lussana, C., and Pianko-Kluczyn ́ska, K.: Observational un- certainty and regional climate model evaluation: A pan-European perspective, International Journal of Climatology, 39, 3730–3749, https://doi.org/10.1002/joc.5249, 2019.

Lange, S.: EartH2Observe, WFDEI and ERA-Interim data Merged and Bias-corrected for ISIMIP (EWEMBI). V. 1.1. GFZ Data Services., http://doi.org/10.5880/pik.2019.004, 2019.

Madakumbura, G. D., Kim, H., Utsumi, N., Shiogama, H., Fischer, E. M., Seland, A., Scinocca, J. F., Mitchell, D. M., Hirabayashi, Y., and Oki, T.: Event-to-event intensification of the hydrologic cycle from 1.5°C to a 2°C warmer world, Scientific Reports, 9, 1–7, https://doi.org/10.1038/s41598-019-39936-2, 2019.

Maúre, G., Pinto, I., Ndebele-Murisa, M., Muthige, M., Lennard, C., Nikulin, G., Dosio, A., and Meque, A.: The southern African climate under 1.5°C and 2°C of global warming as simulated by CORDEX regional climate models, Environmental Research Letters, 13, 065 002, https://doi.org/10.1088/1748-9326/aab190, 2018.

McSweeney, C. F., Jones, R. G., Lee, R. W., and Rowell, D. P.: Selecting CMIP5 GCMs for downscaling over multiple regions, Climate Dynamics, 44, 3237–3260, https://doi.org/10.1007/s00382-014-2418-8, 2015.

NCC editorial: The CMIP6 landscape, Nature Climate Change, 9, 727–727, https://doi.org/10.1038/s41558-019-0599-1, 2019.

O'Neill, B. C., Tebaldi, C., Vuuren, D. P. v., Eyring, V., Friedlingstein, P., Hurtt, G., Knutti, R., Kriegler, E., Lamarque, J.-F., Lowe, J., Meehl, G. A., Moss, R., Riahi, K., and Sanderson, B. M.: The Scenario Model Intercomparison Project (ScenarioMIP) for CMIP6, Geoscientific

Model Development, 9, 3461–3482, https://doi.org/https://doi.org/10.5194/gmd-9-3461-2016, 2016.

Osima, S., Indasi, V. S., Zaroug, M., Endris, H. S., Gudoshava, M., Misiani, H. O., Nimusiima, A., Anyah, R. O., Otieno, G., Ogwang, B. A., Jain, S., Kondowe, A. L., Mwangi, E., Lennard, C., Nikulin, G., and Dosio, A.: Projected climate over the Greater Horn of Africa under 1.5°C and 2°C global warming, Environmental Research Letters, 13, 065 004, https://doi.org/10.1088/1748-9326/aaba1b, 2018.

Ruane, A. C. and McDermid, S. P.: Selection of a representative subset of global climate models that captures the profile of regional changes for integrated climate impacts assessment, Earth Perspectives, 4, 1, https://doi.org/10.1186/s40322-017-0036-4, 2017.

Rubel, F. and Kottek, M.: Observed and projected climate shifts 1901-2100 depicted by world maps of the Köppen-Geiger climate classification, Meteorologische Zeitschrift, pp. 135–141, https://doi.org/10.1127/0941-2948/2010/0430, 2010.

Schneider, U., Becker, A., Finger, P., Meyer-Christoffer, A., Rudolf, B., and Ziese, M.: GPCC Full Data Reanaly- sis Version 6.0 at 0.5: Monthly Land-Surface Precipitation from Rain-Gauges built on GTS-based and Historic Data., https://doi.org/10.5676/DWD_GPCC/FD_M_V7_050, 2011.

Seneviratne, S., Nicholls, N., Easterling, D., Goodess, C., Kanae, S., Kossin, J., Luo, Y., Marengo, J., McInnes, K., Rahimi, M., Reichstein, M., Sorteberg, A., Vera, C., and Zhang, X.: Managing the Risks of Extreme Events and Disasters to Advance Climate Change Adaptation [Field, Barros, Stocker et al. (eds.)], book section Changes in climate extremes and their impacts on the natural physical environment, pp. 109–230, Cambridge University Press, Cambridge, United Kingdom and New York, NY, USA, 2012.

Sun, Q., Miao, C., Duan, Q., Ashouri, H., Sorooshian, S., and Hsu, K.-L.: A Review of Global Precipitation Data Sets: Data Sources, Estimation, and Intercomparisons, Reviews of Geophysics, 56, 79–107, https://doi.org/10.1002/2017RG000574, 2018.

Taylor, K. E., Stouffer, R. J., and Meehl, G. A.: An Overview of CMIP5 and the Experiment Design, Bulletin of the American Meteorological Society, 93, 485–498, https://doi.org/10.1175/BAMS-D-11-00094.1, 2012.

van Oldenborgh, G.J., M. C., Arblaster, J., Christensen, J., Marotzke, J., Power, S., Rummukainen, M., and Zhou, T.: Climate Change 2013: The Physical Science Basis. Contribution of Working Group I to the Fifth Assessment Report of the Intergovernmental Panel on Climate Change [Stocker, T.F. and Qin, D. and Plattner, G.-K. and Tignor, M. and Allen, S.K. and Boschung, J. and Nauels, A. and Xia, Y. and Bex, V. and Midgley, P.M. (eds.)], book section Annex I: Atlas of Global and Regional Climate Projections, pp. 1311–1394, Cambridge University Press, Cambridge, United Kingdom and New York, NY, USA, https://doi.org/10.1017/CBO9781107415324.029, www.climatechange2013.org, 2013.

WMO: WMO Guidelines on the Calculation of Climate Normals. WMO - No. 1203, https://library.wmo.int/doc_num.php?explnum_id= 4166, 2017.

# FIGURES

(a) IPCC WGI Reference Regions (v3, AR5)

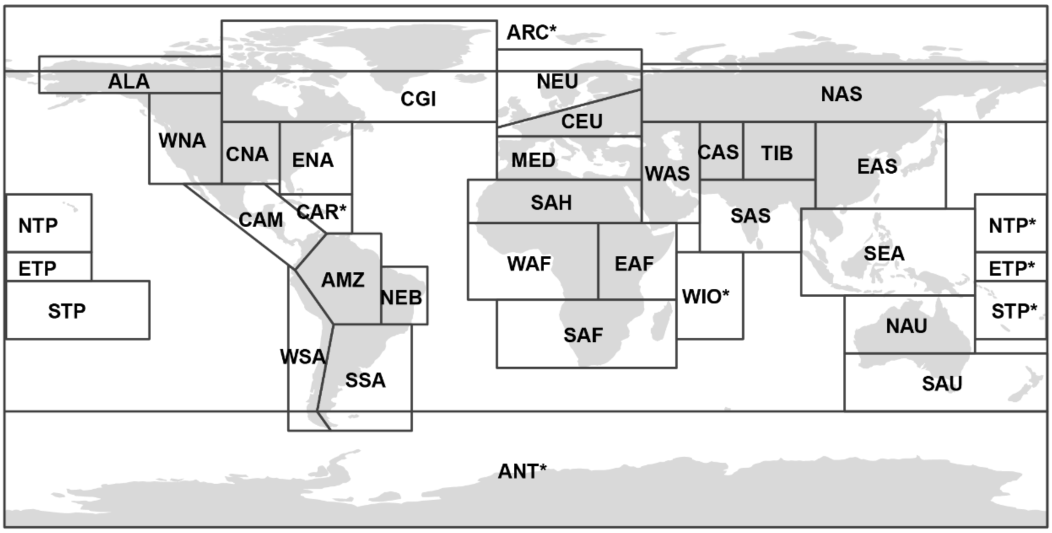

(b) Updated IPCC WGI Reference Regions (v4)

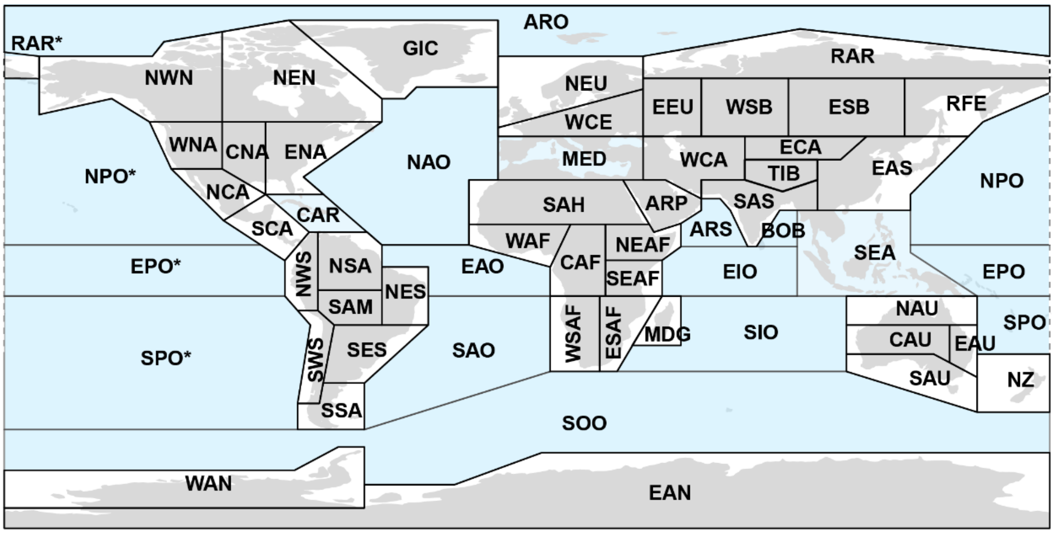

| | | | | | | | | |
|---|---|---|---|---|---|---|---|---|
| 1 | GIC | Greenland/Iceland | 23 | SAH | Sahara | 43 | NAU | N.Australia |
| 2 | NWN | N.W.North-America | 24 | WAF | Western-Africa | 44 | CAU | C.Australia |
| 3 | NEN | N.E.North-America | 25 | CAF | Central-Africa | 45 | EAU | E.Australia |
| 4 | WNA | W.North-America | 26 | NEAF | N.Eastern-Africa | 46 | SAU | S.Australia |
| 5 | CNA | C.North-America | 27 | SEAF | S.Eastern-Africa | 47 | NZ | New-Zealand |
| 6 | ENA | E.North-America | 28 | WSAF | W.Southern-Africa | 48 | EAN | E.Antarctica |
| 7 | NCA | N.Central-America | 29 | ESAF | E.Southern-Africa | 49 | WAN | W.Antarctica |
| 8 | SCA | S.Central-America | 30 | MDG | Madagascar | 50 | ARO | Arctic-Ocean |
| 9-10 | CAR | Caribbean | 31 | RAR | Russian-Arctic | 51 | NPO | N.Pacific-Ocean |
| 11 | NWS | N.W.South-America | 32 | WSB | W.Siberia | 52 | EPO | Equatorial.Pacific-Ocean |
| 12 | NSA | N.South-America | 33 | ESB | E.Siberia | 53 | SPO | S.Pacific-Ocean |
| 13 | NES | N.E.South-America | 34 | RFE | Russian-Far-East | 54 | NAO | N.Atlantic-Ocean |
| 14 | SAM | South-American-Monsoon | 35 | WCA | W.C.Asia | 55 | EAO | Equatorial.Atlantic-Ocean |
| 15 | SWS | S.W.South-America | 36 | ECA | E.C.Asia | 56 | SAO | S.Atlantic-Ocean |
| 16 | SES | S.E.South-America | 37 | TIB | Tibetan-Plateau | 57 | ARS | Arabian-Sea |
| 17 | SSA | S.South-America | 38 | EAS | E.Asia | 58 | BOB | Bay-of-Bengal |
| 18 | NEU | N.Europe | 39 | ARP | Arabian-Peninsula | 59 | EIO | Equatorial.Indic-Ocean |
| 19 | WCE | Western&Central-Europe | 40 | SAS | S.Asia | 60 | SIO | S.Indic-Ocean |
| 20 | EEU | E.Europe | 41-42 | SEA | S.E.Asia | 61 | SOO | Southern-Ocean |
| 21-22 | MED | Mediterranean | | | | | | |

**Figure 1.** Updated IPCC reference land (gray shading) and ocean (blue shading) regions; note that the Caribbean and the Mediterrean are considered both land and ocean regions (defined using the land and sea masks, respectively). Land masks are used to obtain land-only information for land regions (excluding the coastal white regions).

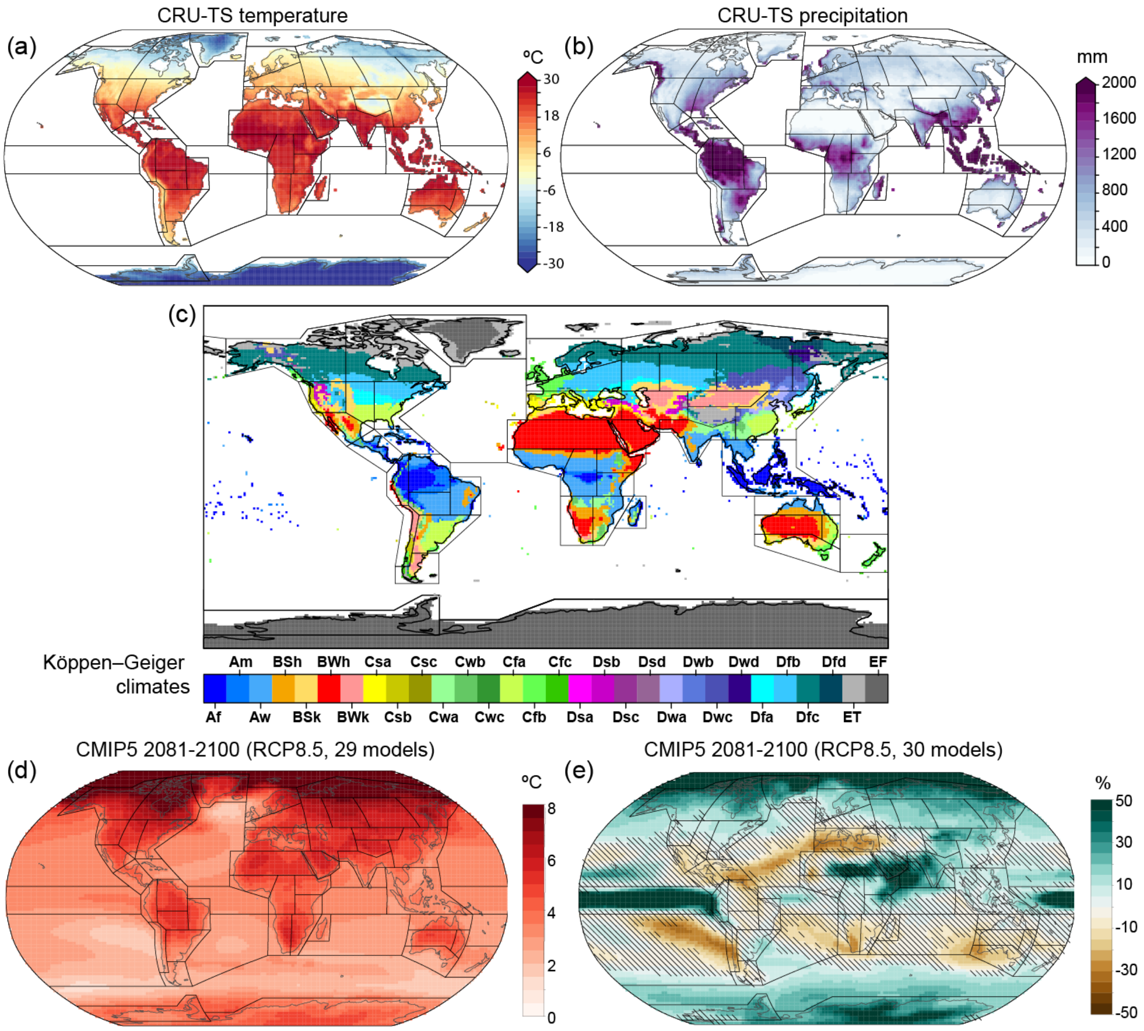

**Figure 2.** (a) Global mean temperature, (b) accumulated precipitation and (c) Köppen-Geiger climate classification from the CRU-TS dataset for the period 1981-2010 (data for Antarctica is filled with the EWEMBI dataset). This information is used to characterize the regional climate consistency of the reference regions (solid lines). (d,e) Climate change projections for temperature and precipitation, respectively, from the CMIP5 curated dataset for RCP8.5 2081-2100 w.r.t. the AR5 modern climate baseline 1986-2005. Hatching indicates weak (less than 80%) model agreement on the sign of the change.

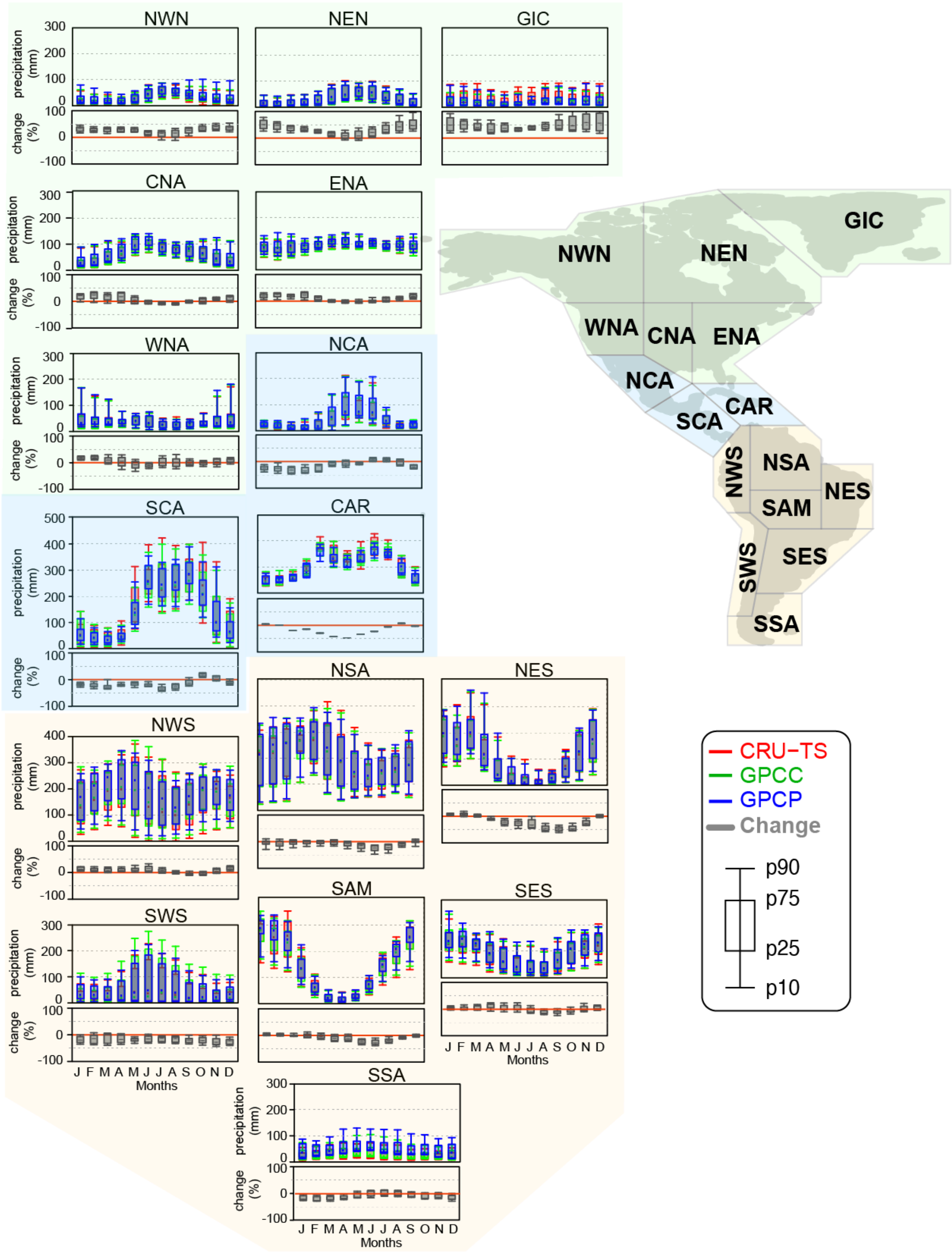

**Figure 3.** Observed annual cycle (1981-2010) for precipitation for the American reference regions from three different observational datasets (CRU-TS, GPCC, GPCP) and climate change signal (RCP8.5, 2081-2100 w.r.t. the AR5 modern climate baseline 1986-2005). The panel for each reference region shows the observed annual cycle (top, in monthly accumulated mm) and the monthly projected changes (bottom, in gray, as %); box and whiskers plots represent the spatial (gridbox) spread of monthly values over the region.

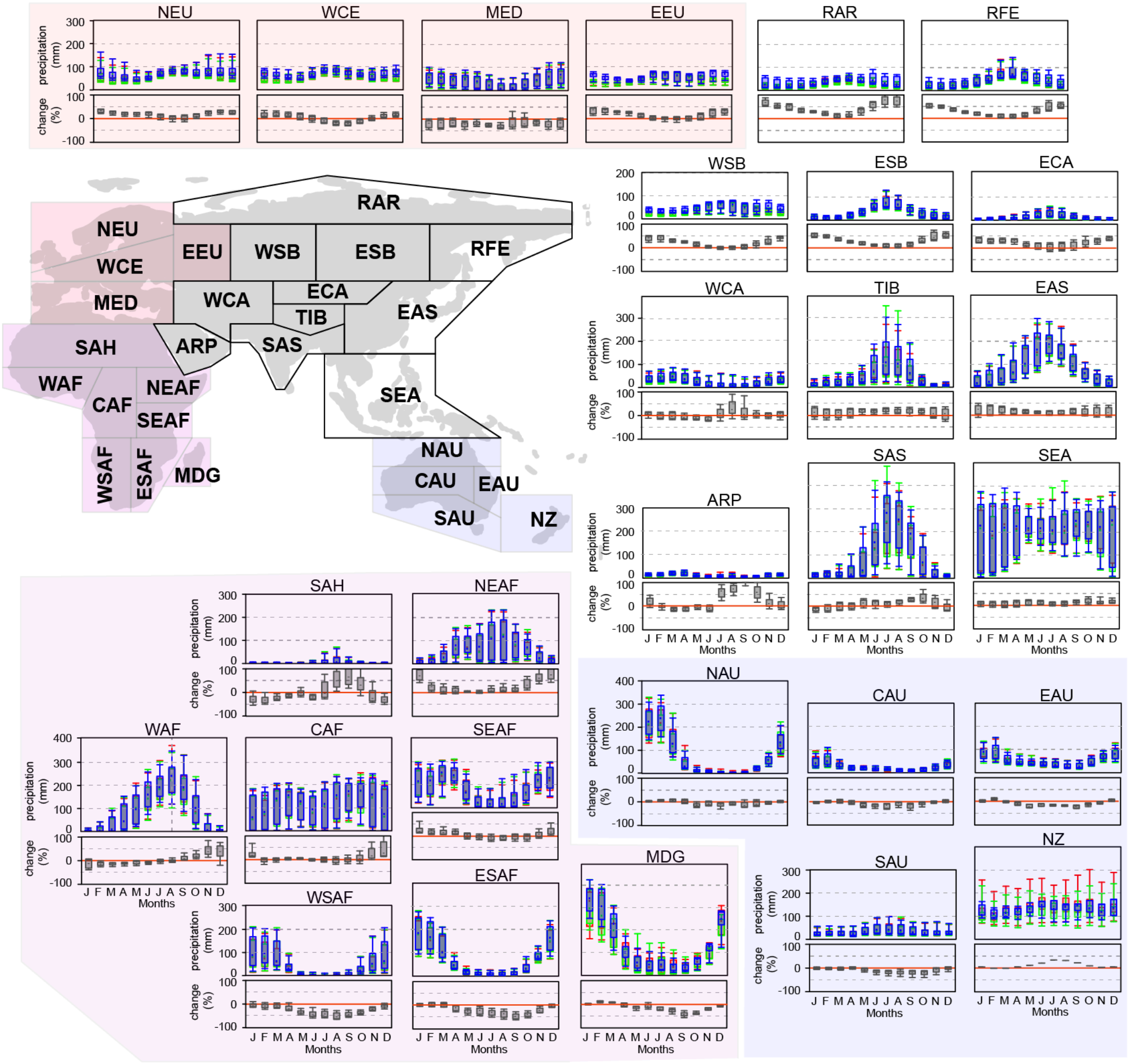

**Figure 4.** As figure 3 but for Europe, Asia and Australasia.

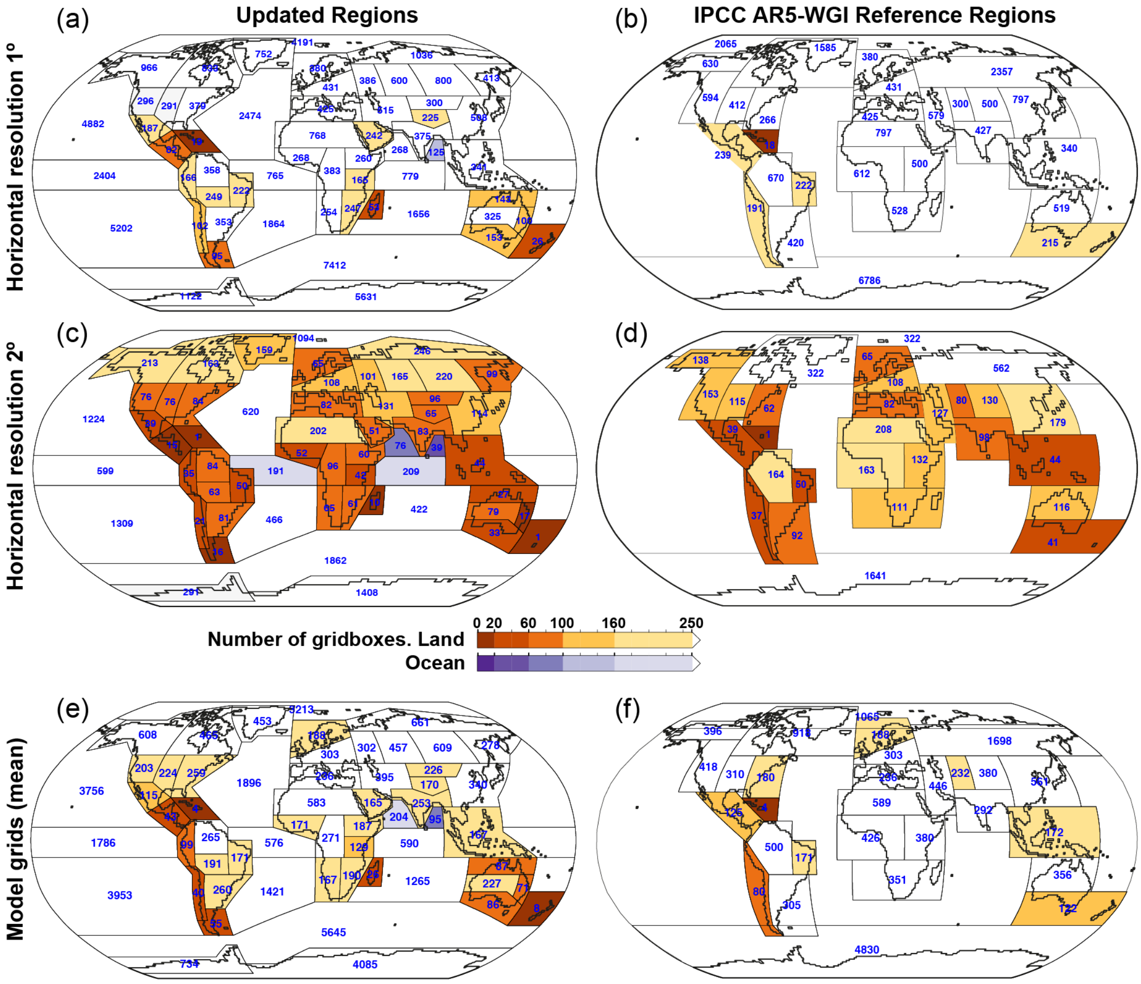

**Figure 5.** Number of gridboxes encompassed by the different reference regions for 1º (a,b) and 2º (c,d) resolution and for the CMIP6 model grids (e,f) –the multi-model mean is represented–, considering the updated (a,c,e) and the original AR5 (b,d,f) reference regions. Colors indicate regions with less than 250 gridboxes. The blue numbers in each of the regions show the number of gridboxes (only land gridboxes for land regions).

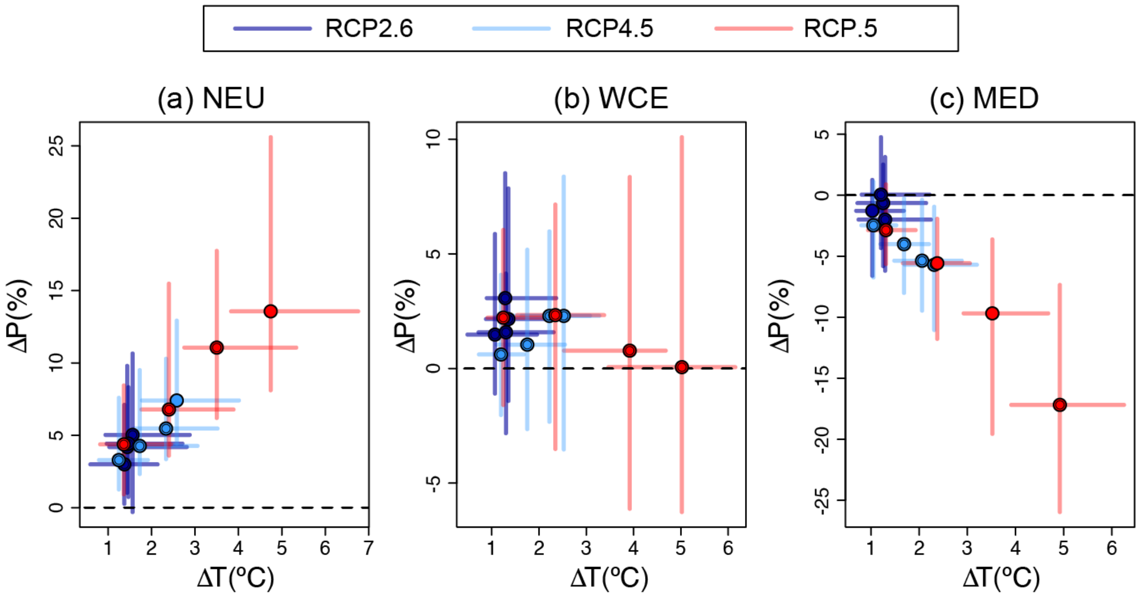

**Figure 6.** Illustrative example of the use of reference regions and aggregated CMIP5 datasets: Regional mean changes in annual mean temperature and precipitation for three European regions (NEU, WCE and MED) for four future periods (2021-2040, 2041-2060, 2061- 2080, 2081-2100), as obtained from CMIP5 projections. Changes are absolute for temperature and relative for precipitation. Horizontal and vertical error bars represent ±1 standard deviation from the mean calculated across the ensemble of included models. The script to generate this figure for all the 61 land and ocean regions (as well as the global results) from the aggregated and ready-to-use CMIP5 datasets is available at the ATLAS GitHub, and can be adapted to produce similar results for alternative datasets (e.g. CMIP6).